Engineering Universe for scientific Research and management
ISSN (Online): 2319-3069
Vol. XV Issue I
January 2023

An Extreme Application of Wide-Band Gap Semiconductors Devices in Power Electronics

Shobha Kumari[1], Ms. Alka Thakur[2]
M.Tech. Scholar, Department of Electrical Engineering, Sri Satya Sai University of Technology and Medical Sciences, Sehore, Madhya Pradesh, India[1]
Associate Professor, Department of Electrical Engineering, Sri Satya Sai University of Technology and Medical Sciences, Sehore, Madhya Pradesh, India[2]

Abstract

Wide-bandgap (WBG) semiconductor materials such as silicon carbide (SiC) and gallium-nitride (GaN) allow higher voltage ratings, lower on-state voltage drops, higher switching frequencies, and higher maximum tempera- tures. All these advantages make them an attractive choice when high-power density and high-efficiency converters are targeted. Two different gate-driver designs for SiC power devices are presented. First, a dual-function gate-driver for a power module populated with SiC junc- tion field-effect transistors that finds a trade-off between fast switching speeds and a low oscillative performance has been presented and experimentally ver- ified. Second, a gate-driver for SiC metal-oxide semiconductor field-effect transistors with a short-circuit protection scheme that is able to protect the converter against short-circuit conditions without compromising the switch- ing performance during normal operation is presented and experimentally validated. The benefits and issues of using parallel-connection as the design strategy for high-efficiency and high-power converters have been presented. In order to evaluate parallel connection, a 312 kVA three-phase SiC inverter with an efficiency of 99.3 % has been designed, built, and experimentally verified. If parallel connection is chosen as design direction, an undesired trade-off between reliability and efficiency is introduced. A reliability analysis has been performed, which has shown that the gate-source voltage stress determines the reliability of the entire system. Decreasing the positive gate-source voltage could increase the reliability without significantly affecting the efficiency. If high-temperature applications are considered, relatively little attention has been paid to passive components for harsh environments. This thesis also addresses high-temperature operation. The high-temperature performance of two different designs of inductors have been tested up to 6000C. Finally, a GaN power field-effect transistor was characterized down to cryogenic temperatures. An 85 % reduction of the on-state resistance was measured at −195◦C. Finally, an experimental evaluation of a 1 kW single- phase inverter at low temperatures was performed. A 33 % reduction in losses compared to room temperature was achieved at rated power.

Keywords: *Wide-bandgap (WBG), Silicon Carbide (SiC), Gallium-Nitride (GaN), Inverter, MOSFET, High Temperature.*

1. Introduction

In general terms, power electronics is the application of solid-state electro- nics components with the task of processing, controlling, and converting electrical energy. Power electronics converters are typically very efficient for various conver- sions of voltages, currents or frequencies. Due to this and a good cost-performance ratio, power electronics converters can be found in many applications [1]. These converters may have different power range, from watts to megawatts according to the needs, and they are subdivided depending on the application. It is possible to identify four types of converters according to the type of conversion they perform. The first one is the commonly known rectifier, which converts from alternating cur- rent (ac) to direct current (dc). This converter is used for almost every consumer electronic device, in order to supply power to the digital electronics. The second type of converter is the so-called inverter, which converts from dc/ac. Inverters can be found in many applications (from industry to traction) in order to supply power to electric drives. To date, this type of converter is also used by renewable energy sources in order to feed the produced power into the electrical grids. The remain- ing types of converters, ac/ac converter and dc/dc converter, are used also in many different applications, such as renewable energy and battery chargers, respectively.

The solid-state electronics components, which are built with power semi- conductor devices, work as switches and are the main part of these power converters. The most common solid-state components are the diodes, thyristors, and transis- tors. In particular, transistors can be categorized as bipolar junction transistors (BJTs), junction field-effect transistors (JFETs), metal oxide semiconductor field- effect transistors (MOSFETs), and

insulated-gate bipolar transistors (IGBTs). The IGBT combines the simple gate-drive characteristics of MOSFETs with the high- current and low-saturation-voltage capability of the BJTs. Therefore, the IGBT is the most used transistor in medium- to high-power applications (10 kW - 1 MW). They can be found in many applications such as variable-frequency drives (VFDs). electric cars, and trains. Furthermore, transistors could also be categorized by the semiconductor material they are composed of. For years, silicon (Si) has been the semiconductor material of excellence. However, new promising technologies have emerged. The wide-band gap (WBG) semiconductor materials such as silicon car-bide (SiC) and gallium–nitride (GaN) allow higher voltage ratings, lower voltage drops, higher switching frequencies, higher thermal conductance, and higher maxi- mum temperatures. All these advantages offered by the WBG semiconductors, in comparison with the currently and commonly used Si, make them an attractive choice when high power density and high efficiency is needed.

Nowadays, many companies are able to manufacture WBG power devices with sufficiently high quality and cost that allows the introduction of these devices on the market. Following the reduction in manufacturing cost for WBG power semiconductors, significant advantages can be achieved in the aforementioned ap- plications, and in some cases the introduction of WBG semiconductors might take power electronics to new areas of development [2].

When SiC power devices were firstly introduced, various quality and perfor- mance related issues were present such as parameters spread. In order to achieve high production yields, these SiC power devices employed chips with comparably small areas, which resulted in low current ratings for discrete devices. Thus, single discrete components could not be used for high-power applications, above tens of kilovolt-amps (kVA). In the literature, two different solutions to reach high current ratings can be found: either to parallel-connect several single-chip discrete devices or to build multi-chip power modules [3–7]. It is important to note that parallel connection not only increases the total current rating but also increases the overall efficiency of the system. Parallel-connecting devices reduces the equivalent on-state resistance, therefore, reducing the on-state losses. However, parallel-connection of transistors may also give rise to adverse effects. Specifically, it has been shown that problems associated with the “Miller effect” might affect stable operation [8]. In particular, the Miller effect may cause accidental turn-ON and self-sustained oscillations between the Miller capacitance of the parallel-connected devices and the stray inductances of the external circuit layout and of the circuit layout of the module as such [8]. Slowing down the switching times would avoid these issues. However, this would mean that the full potential of the WBG technology could not be taken as an advantage.

Another possibility to reach even higher power ratings (of the order of hun- dreds of kVA) is the parallel-connection of power modules. This could bring the benefits of the WBG technology to further applications. By successfully achieving parallel-connection (either discrete components, or power modules) and fast switch-ing performance the final design would benefit from both high switching frequencies and a high current capability.

Unfortunately, increasing the amount of components, such as parallel connec- tion of devices, may have a negative impact on the reliability of the system. By introducing additional components the probability of failure increases. Therefore, an undesired trade-off between the targeted high current ratings and high efficiency, and the reliability of the system is introduced. Finally, all these benefits also make the WBG semiconductors ideal candidates for power electronics systems under harsh environments. These harsh environments could be either extreme high temperature applications (600oC), such as automotive, oil and gas drilling, and space applications (Venus explorations) [9–11] or extreme cold environments such as future electric aircrafts, where cryo-cooling is considered for ultra-light superconducting electric machines [12–14].

Many issues on design, fabrication, driving, and reliability of WBG power devices and their applications are still waiting for answers. This thesis aims to contribute with solutions for various issues regarding extreme implementations of WBG semiconductors in power electronics.

2. SiC and GaN Power Devices

The significant achievements in both SiC bulk material growth and process technology provide an excellent scenario to this semiconductor material for high-power applications. High quality SiC wafers are mandatory for a reasonable yield of large-area SiC power devices. The progress is reflected in the achievement of very low micropipe density (0.75 cm^{-2} for a 75-mm wafer). Today, 100-mm SiC wafers are in the market, and 150-mm SiC wafers will be available in a near future [15]. Apart from micropipe formation, other defects causing poor reliability in bipolar devices, such as basal plane dislocations, are still under investigation.

A. SiC Power Rectifiers

In comparison with Si counterparts, a ×10 increase in blocking voltage is possible with the same SiC drift layer thickness due to the SiC larger dielectric critical field. The high thermal conductivity of SiC is also a great advantage in comparison with Si diodes since it allows operating at higher current density ratings as well as to minimize the size of the cooling systems. There are basically three types of SiC power rectifiers [16], their cross sections being shown in Fig. 1:

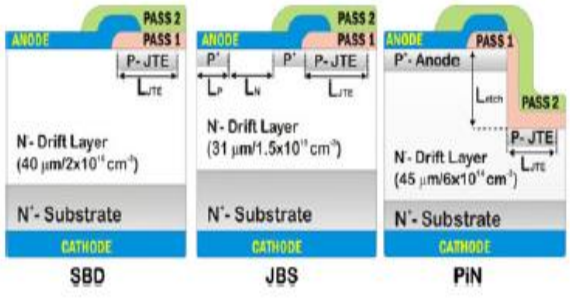

Fig. 1. Cross section of 4H-SiC 3.3-kV Schottky, JBS, and p-i-n diodes [4].

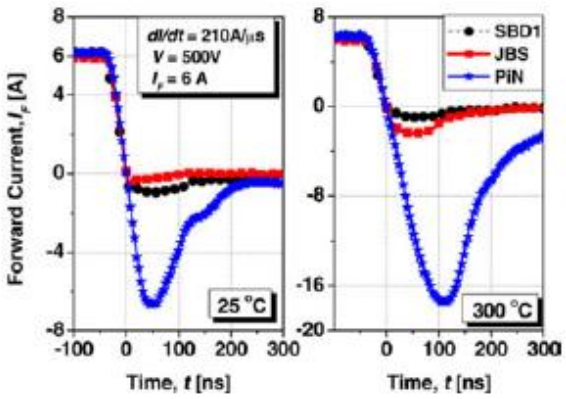

Fig. 2. 3.3-kV SiC diodes turn-off current waveforms at 25 ◦C and 300 ◦C with inductive load [17].

1) Schottky Barrier Diodes (SBDs) showing extremely high switching speed and low on-state losses, but lower blocking voltage and high leakage current;
2) p-i-n diodes with high-voltage operation and low leakage current, but showing reverse recovery charging during switching;
3) Junction Barrier Schottky (JBS) diodes with Schottky-like on-state and switching characteristics, and p-i-n-like offstate performance. SiC SBDs are commercially available since 2001 and have shown a continuous increase in the blocking voltage and conduction current ratings. Concretely, they range from the initial 300 V/10 A and 600 V/6 A to the actual 600 V/20 A and 1.2/1.7 kV with current capabilities as high as 50 A [18], [19], these ratings being further increased in the near future. In fact, commercial 3.3-kV Schottky diodes have been already announced [20], and it is expected that they will eventually replace Si p-i-n rectifiers in the 600 V–3 kV range. Moreover, the easy SBD paralleling has allowed the introduction of commercial IGBT 600 A/1.2 kV power modules containing SiC SBDs as freewheeling diodes [21]. The ability of SiC devices for high-temperature operation makes them suitable for many applications in aerospace and space missions [22] although high-temperature reliable device packaging needs to be developed [23], [24]. Large-area 3.3-kV SBDs have been fabricated for high-temperature applications [4] with forward currents in the range of 10–20 A. An example of high-temperature operation is the 300-V, 5-A SBD diodes developed for harsh environment space applications (BepiColombo ESA mission) [25]. Besides, SiC SBDs are well suited for high switching speed applications due to the low reverse recovery charge in comparison with ultrafast Si p-i-n diodes. Thus, SiC SBDs match perfectly as freewheeling diodes with Si IGBTs. Fig. 3 displays the reverse recovery of the three SiC rectifiers at 25 ◦C and 300^0C.

Hybrid rectifiers, merging p-i-n and Schottky structures (JBS diodes), are particularly attractive since they combine the benefits of a high blocking voltage capability from p-i-n diodes and the low reverse recovery of SBDs (see Fig. 2). They are commercially available up to 1.2 kV, and Infineon has recently presented the thin Q!TM 5G generation [26] of 650-V JBS diodes based on a thin-wafer technological process showing improved surge current capability and avalanche ruggedness with a positive temperature coefficient. Besides, high-current (50 A) JBS diodes for being used as antiparallel diodes in IGBT modules are available from Cree, and 75 A–100 A/1.2 kV up to 20 A/10 kV JBS diodes have also been demonstrated [27]. Due to reliability problems (forward voltage drift mainly), there are no SiC bipolar diodes available in the market. Nevertheless, SiC state-of-the-art p-i-n diodes include that reported in [28] with a forward voltage drop of 3.2 V at 180 A (100 A/cm2), and a blocking voltage capability of 4.5 kV with a reverse leakage current of 1 μA. In fact, p-i-n diodes will only be of interest for breakdown voltages over 2–3 kV, and structures with blocking capability up to 20 kV have been demonstrated [29]. However, their commercialization will depend on overcoming reliability problems through the improvement of the starting semiconductor material quality.

B. GaN Rectifiers

GaN is particularly attractive for high-voltage, high frequency, and high-temperature applications due to its WBG, large critical electric field, high electron mobility, and reasonably good thermal conductivity. At present, GaN-based devices are already commercialized in the photonics area, while this semiconductor material is still in a first stage concerning power applications. Due to the lack of commercial high-quality freestanding GaN substrates in the past, GaN epilayers have been mainly grown on foreign substrates, particularly, SiC, sapphire, and Si. Growing high-quality, single-crystalline GaN films, which are essential for the power conversion, requires a welldefined
global epitaxial relationship between the epitaxial GaN film and the substrate. Among the diverse possibilities, GaN epilayers grown on Si substrates offer a lower cost technology compared to the other substrates as well as allowing material growth on large diameter substrates up

to 200 mm [30]. Most of GaN Schottky power diodes reported up to now are either lateral or quasi-vertical [31] structures due to the lack of electrically conducting GaN substrates. Breakdown voltages of lateral GaN rectifiers as high as 9.7 kV have been obtained on Sapphire substrates [32] although the forward voltage drop is still high. GaN rectifiers implemented on Si or Sapphire substrates are attracting a lot of attention because of their lower cost. Recently, with the availability of high-temperature hydride vapor phase epitaxy free-standing GaN substrates, 600-V GaN Schottky diodes are due to be launched in the market to compete with SiC Schottky rectifiers [33]. In addition, commercial GaN Schottky diodes will be available in the market in a very near future in the 600 V–1.2 kV voltage range. On the other hand, JBS GaN diodes are also being investigated which could further increase the performance of GaN-based power rectifiers in the 600 V to 3.3 kV range, although improvements in the contact resistance to implanted p-type GaN are still needed [34].

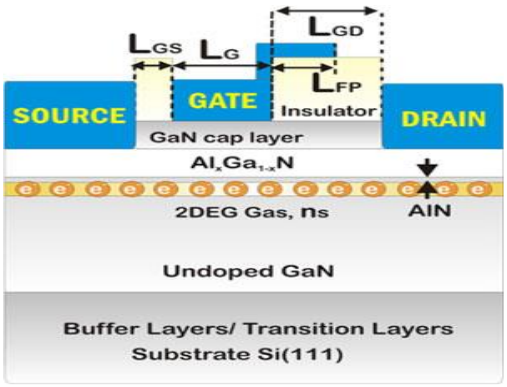

Fig. 4. Cross section of a normally-on GaN HEMT [35].

3. Applications of Wide-Bandgap Power Devices

As previously mentioned in this chapter, several applications have identified the advantageous characteristics that come inherently with the WBG semiconduc- tors. In this section a more detailed description on how these applications have benefited from using WBG technology is presented.

When the SiC power devices were introduced on the market, their only com- petition was the commonly used Si IGBTs. This was mainly due to the 1200 V rated voltage. Some examples of these applications are:

- Power Factor Correction as shown in [36]. For this application the drop-in replacement of the power switch was enough to produce an increase in total system efficiency. Combining these results with the ability of the SiC devices to achieve higher switching frequencies will potentially lead to smaller, and more efficient power electronic circuits.
- Micro-Grids with distributed generation could reduce the emissions and green house effect. Nevertheless, power converters using Si are comparably bulky and not sufficiently efficient for this application. SiC high-voltage power devices could become key components in order to achieve this kind of system. As shown in [37], the higher switching frequency and reduced voltage drop will contribute to smaller and more efficient converters.
- Renewable Energy Power Sources (Solar Power, Wind Power, etc.) can experience a system's size and cost reduction due to the improvement in conversion efficiency (99 %), high frequency operation, and high temperature properties of the SiC devices [47]. As shown in [39], these benefits can be obtained with a one-for-one replacement without any further optimizations.
- Modular Multilevel Converters (MMC) using SiC switches could have many benefits, including diode-less operation [39,40]. In [41], this is presented and verified assuring the feasibility of using SiC JEFTs. Moreover, efficiencies of 99.8 % are expected for a 300 MW MMC used in HVDC.
- Power Inverters with efficiencies well above 99 % are more than possible us- ing SiC power devices. In [42], a 40 kVA inverter with an efficiency exceeding 99.5 % using natural convection cooling is presented.
- Data Center power supplies could also profit as presented in [43] with ultra high-efficiency buck rectifiers.
- Automotive applications will gain due to the high-temperature capability, high power density, and high efficiency offered by SiC devices. If high power density converters are considered even more benefits could be associated to the use of SiC devices [44–46]. Properties such as weight and volume affect directly the whole power train system design and cost in the electric and hybrid vehicles.
- Resonant Converters for induction heating and other applications is also an area that has perceived the benefits of using SiC. In particular, there are control techniques, such as dual control proposed that are now feasible using SiC devices as replacement for the commonly used Si IGBTs.
- Space Applications, in particular for harsh environments, such as Venus explorations, SiC has shown a great potential. The high-temperature ca- pability makes the SiC power devices ideal candidates for this application. In , the performance of the SiC JFETS operating at temperatures up to 450 oC is presented. The SiC power device is able to operate within the entire temperature range without significant adverse effects.

Furthermore, the GaN power devices have a voltage rating in the range from 15 to 300 V, which make them a direct competitor with the currently used Si MOSFETs. Even though the GaN power FET was introduced only recently to the market, their benefits are clear in many applications, such as:

- dc/dc Conversion using GaN devices will enable high efficiencies and high switching frequencies due to their low on-state resistance and low gate capaci- tance, respectively. In a dc/dc boost converter with a switching frequency of 10 MHz and an efficiency above 90% is presented. Moreover, techniques such as dead time optimization are also feasible using GaN switches.
- In an inverter using GaN power switches operating at 10's of MHz for Wireless Power Transfer is presented. The combination of the low induc- tive package, the fast switching capability, the low gate capacitance, and the low on-state resistance make the GaN device the ideal component for this application [47].
- Power Inverters used in many applications such as solar power generation and other appliances are desired to have high efficiency and to be compact. In a 2 kW single-phase inverter is presented. The inverter presents a 7-level flying capacitor multilevel topology using GaN switches operating at 120 kHz, while maintaining an efficiency above 99 %. The low-loss characteristics of the GaN power switches enable using non-typical topologies for these applications, which could bring additional benefits not present yet.
- Other applications such as Envelope tracking, Light Distancing and Ranging (LiDAR), and Class D audio amplifiers could benefit from the low losses enabling higher efficiencies. These systems could produce less heat, save space and cost, and extend the battery life in portable systems.

There are even more applications than the ones aforementioned that are tak- ing advantage of the WBG semiconductors properties. This also shows that the technology has matured to some extent and exploring its limits through extreme implementations is a natural step forward.

4. Methodology

As mentioned above, the main target is to achieve a high efficiency (> 99 %) at a relatively high switching frequency (20 kHz) for a three-phase two-level VSC. The electric parameters of the converter are shown in Table 1. Furthermore, parallel-connection of power modules was chosen as a solution for the design methodology of the converter. This will increase the total chip area and decrease the total equivalent on-state resistance. Thus, the expected conduction losses will be reduced.

Table 4.1: Electrical Parameters of The Three-Phase Inverter.

Power Rating, S_n	312 kVA
Input Voltage	650 VDC
Output Voltage (Line-to-Line)	400 VRMS
Output Current(Phase)	450 ARMS
Switching Frequency, f_{sw}	20 kHz
DC Capacitance, C	720 µF
Blanking Time	600 ns

Based on the electrical parameters required for the industrial application it was decided to connect ten power modules in parallel per phase-leg. Based on calculations, with this number of modules, the expected on-state power losses are expected to be within 0.3 % and 0.4 % of the nominal power, Sn. This is a reason-able value considering that the total losses should be lower than 1 %. Additionally, a negative temperature coefficient of the conduction losses below 40oC is revealed in Figure 5. However, with ten power modules connected in parallel at the rated output power, the current of each power module is sufficiently high so as to in- crease the junction temperature to be where the on-state resistance is well within the positive-temperature-coefficient range. This is necessary in order to activate the auto-balancing mechanism of the current sharing among the parallel-connected power modules. Moreover, an even number of power modules is crucial for the system complexity and the symmetrical placement. The symmetrical placement will reduce the spread in the parasitic elements of the external circuit layout, thus, contributing also to an even current sharing. Ten parallel-connected power modules find a compromise between low on-state power losses, current density, and system complexity. Finally, it must be noted that the power modules used in this part of the work were chosen without any sorting whatsoever.

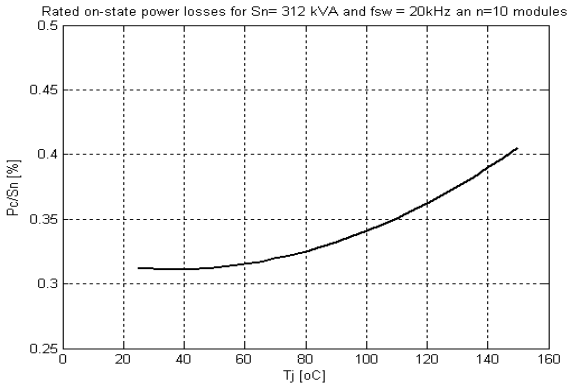

Fig. 5: Relative on-state power loss versus junction temperature for ten parallel- connected modules (CAS100H12AM1) - calculation using datasheet values.

Taking into consideration the physical dimensions of the power modules shown in Figure 6, the circuit layout of the complete three-phase converter, built with ten parallel-connected SiC power modules per phase-leg, is shown in Figure 7. The previously mentioned symmetrical placement of the power modules was achieved using U-shaped bus bars in each phase-leg. Moreover, in order to further reduce the parasitic stray inductances of the external circuit layout, the positive and negative bus bars were placed on top of each other. Thus, the stray inductance introduced by the magnetic field generated with the flow of current, will partially be canceled as shown in Figure 8. The figure shows in blue and red the magnetic field generated by the positive (bottom) and negative (top) bus bars, respectively.

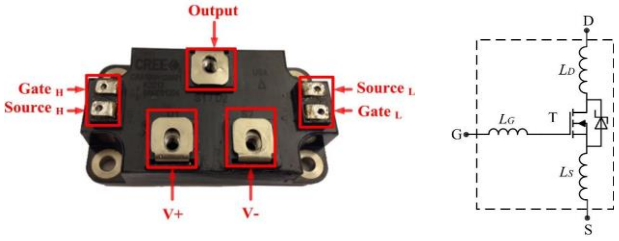

Figure 6: (a) Photograph of the power module with SiC MOSFETs and, (b) Simplified schematic diagram of a single switch position.

Moreover, the dc-capacitance has been distributed throughout the bus bars. This ensures the lowest stray inductance from the source of energy to each power module. Additionally, several interconnections between the prototype and the power supply were made in order to ensure that the distributed capacitors behave as a single capacitor. This is important in order to ensure a uniform distribution of the current among the distributed capacitors, including the 2nd order harmonic.

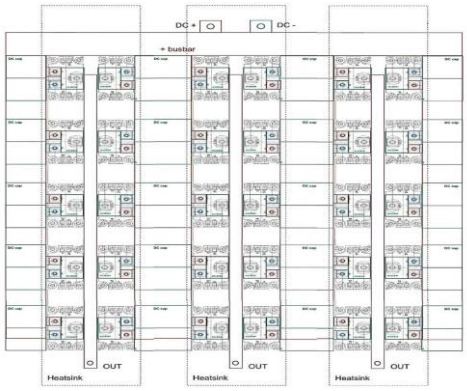

Fig. 7: Schematic diagram of a single phase set-up.

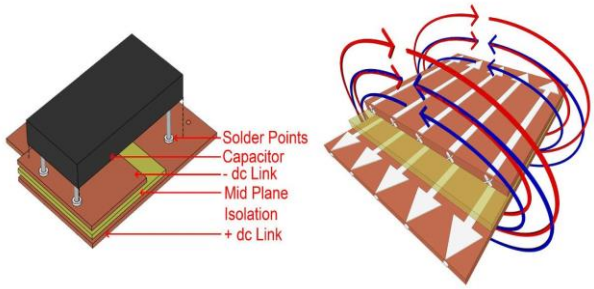

Fig. 8: Layout of the bus bars for the inverter.

Finally, distributed single gate-drive units were connected independently to each gate lead of the power module. This reduces the gate loop inductance, which in con- junction with the Miller capacitance determines the stability of the system, and the switching speeds. A photograph of the partially built prototype for the three-phase system with the proposed methodology, bus-bars system and distributed capacitors is shown in Figure 9.

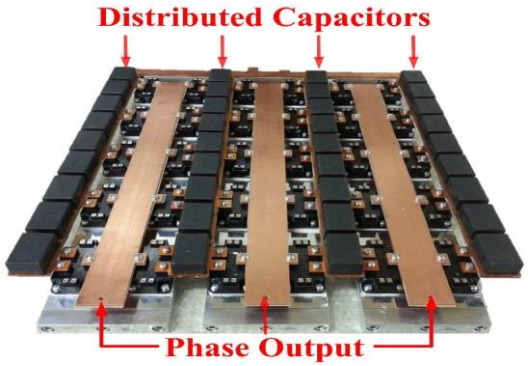

Fig. 9: Photograph of the partially built three-phase inverter

By successfully reaching fast switching speeds, a high efficiency could be achieved with the chosen switching frequency. A high switching frequency such as 20 kHz reduces the required dc-link capacitance, which simplifies the task of distributing the total capacitance throughout the complete bus-bars system. Fi- nally, it is important to note that a suitable choice of power modules is crucial for the final design. Low-current-rated power modules that can switch faster than higher-current-rating ones (as the SiC JFET power modules presented in the pre- vious chapter) in combination with a successful parallel connection will enable a fast switching performance and high current capability.

5. Experimental Results

The experimental verification of the proposed methodology was performed in two steps. First, a single-phase prototype was designed, built, and tested. This test was subdivided into three sub-steps. A

transient analysis was done with a DPT, an steady-state analysis was performed using the single-phase prototype as a dc/dc converter, and finally, a thermal analysis was performed. Second, the complete three-phase VSC was designed, built, and tested at different output powers up to the rated load. Moreover, in order to minimize the power dissipated in the testing facilities, this last part of the test was performed using an inductive load. The dissipated power was fed by a dc power supply.

Experimental Evaluation of the Single-Phase Prototype

As previously mentioned, the experimental evaluation of the single-phase pro- totype was performed using a DPT. Figure 4.5a shows a schematic diagram of the experimental set-up. This set-up consists of a dc capacitor, C, connected with a dc-power supply, V_{DC}, and a load, which is an air coil inductor, L, and its resis- tance represented by R. The values of the parameters used in the experimental set-up are shown in Table 4.2. A photograph of the single phase leg is shown in Figure 4.5b. The flying wires shown in the photograph are power cables for the individual gate-drive units for each power module and optical fibers between the micro-controller and the gate drivers of the power modules.

Table 4.2: Parameters of the Experimental Set-Up of the DPT.

DC supply voltage, V_{DC}	700 V
Inductance, L	70 μH
Capacitance, C	560 μF

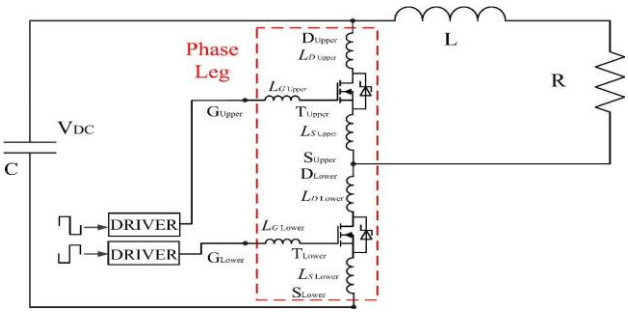

(a)

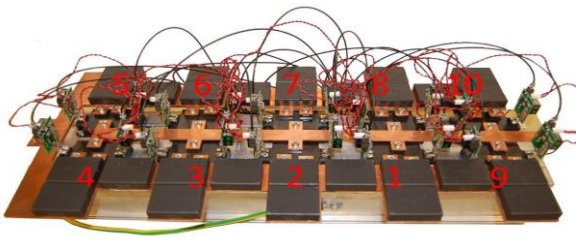

(b)

Figure 4.5: (a) Schematic diagram of the double-pulse test set-up, (b) Photograph of the prototype.

Transient Analysis

For the DPT the dc-power supply was set to 700 V. Figure 4.6 shows the current sharing of the power modules. It can be noted that the power modules No. 1 and No. 8, conduct significantly higher currents than other power modules, especially power module No. 6. There are several possible explanations to this phe- nomenon. One possible reason is the closer placement of power modules No. 1 and No. 8 to the output of the phase-leg prototype, which means a lower stray parasitic inductance. Another reason could be a mismatch between the device characteristics of the SiC MOSFET power modules, such as the transconductance or on-state resistance. Nevertheless, except for power module No. 6, the remaining power modules share the static current with a maximum difference of 25 %.

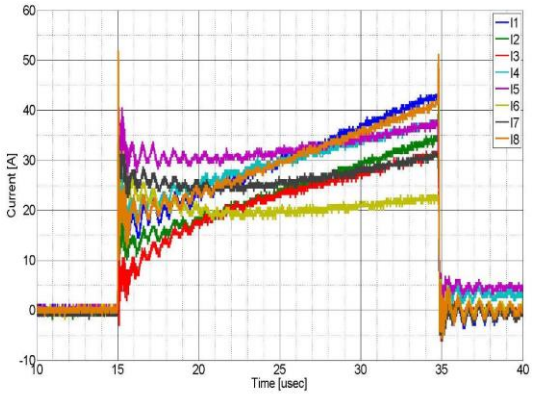

Figure 4.6: Current sharing of the SiC MOSFETs. Measured drain current of each SiC power module.

Moreover, a closer evaluation was performed of the switching transients. Fi- gure 4.7a shows the turn-ON transient, which takes approximately 35 ns. During this period the current sharing is acceptably uniform. On the other hand, Fi- gure 4.7b shows the turn-OFF transient, which takes approximately 50 ns. The turn-OFF current sharing is reasonably uniform for all the modules except for power modules No. 2 and No. 8. It is the hypothesis of the author that the over- shoots in the currents of these power modules, as shown in Figure 4.7b, are due to a mismatch in the characteristics of the MOSFET power modules. Specifically, a difference in threshold voltage among the power modules will cause the power mo- dules to turn OFF at different instants. Thus, an increase in the currents of these power modules is expected. This behavior will cause a difference in turn-OFF losses among the power modules, which could lead to early failures or reliability issues.

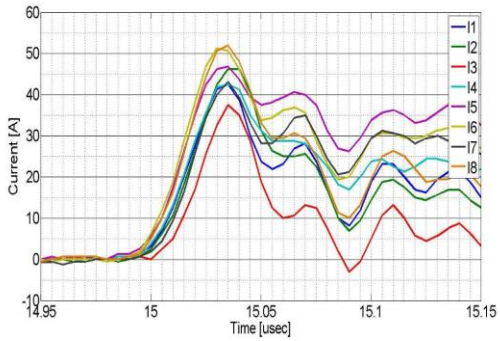

(a)

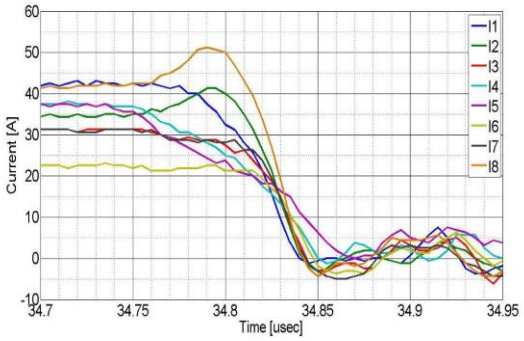

(b)

Figure 4.7: Measured drain current of each SiC power module. (a) Turn-ON tran- sient of the SiC MOSFETs. (b) Turn-OFF transient of the SiC MOSFETs.

Steady-State Analysis

For the steady-state analysis, the previously presented experimental set-up was connected as a dc/dc converter. The duty ratio was set to 0.1 and using the air coil inductor as the load itself. *V*DC was increased until the output current reached 450 A, i.e. nominal output current. Figure 4.8 shows the results during steady-state operation. The current sharing of modules No. 2, No. 4, No. 6 and No. 8 was observed. The steady-state current is approximately 45 A per module. With this higher current, it is possible to notice the difference in the on-state resistances between the modules. Specifically, the steady-state current in module No. 8 is 40 A, which indicates a higher on-state resistance than the other three modules, transient analysis. This is mainly due to the continuous operation, which increases the temperature of operation. The increased temperature of operation causes the power modules to operate well within the positive-temperature-coefficient range of the on-state resistance, which results in an auto-balancing mechanism of the module currents.

A closer look to the switching transients was performed. Figure 4.9a shows the turn-ON transient of the currents.

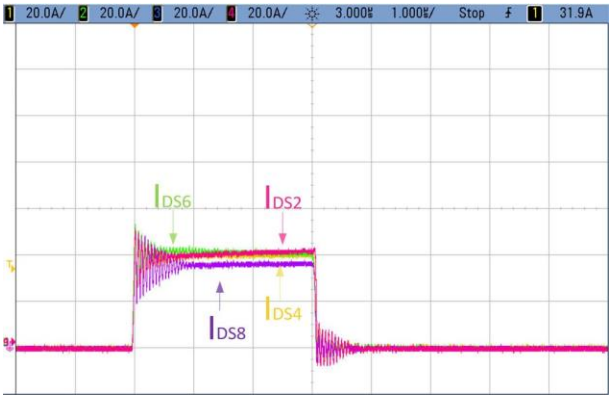

Figure 4.8: Current sharing of the SiC MOSFETs. Measured drain current of each SiC power module.

The turn-ON process takes approximately 50 ns and the current sharing is more uniform than in the transient analysis case. Figure 4.9b shows the turn-OFF transient, which takes approximately 50 ns as well with a current sharing that is also more uniform than in any of the previous cases. Moreover, it is possible to note a delay in the turn-OFF process of the current in Module No. 2. This could be due to several reasons such as a mismatch in the MOSFET power module characteristics or a difference in the stray inductances of the interconnections of the modules. Moreover, an additional possible reason would be a difference in the current measurement probes.

5. Conclusion

When parallel-connection is chosen as the design methodology of high-efficiency converters rated for high-power applications, special considerations need to be taken into account regarding the parasitic components of the set-up. By ensuring a low inductive set-up and properly selecting the power modules, a uniform distribution of the currents among the power modules as well as a fast switching performance could be achieved. These elements affect directly the switching losses and, there- fore, the efficiency of the system. Moreover, a more uniform distribution of the currents was recorded at high powers than at low powers. It is believed that the positive-temperature-coefficient of the on-state resistances works as an auto- balancing mechanism of the current sharing among the parallel-connected power modules. A 312 kVA three-phase SiC inverter with high efficiency has been designed, built, and experimentally verified using parallel-connection as construction metho-dology. From the measurements, the total losses of the main circuit were found to be 2.29 kW at 312 kVA, which corresponds to an efficiency of 99.3 %. The key to reach such a high efficiency was a combination of a successful massive parallel- connection of SiC power modules, using diode-less operation, and high switching speeds.

Reference

[1] N. Mohan, T. M. Undeland, and W. P. Robbins, *Power Electronics. Convert- ers, Applications and Design*. John Wiley and Sons, Inc, Third ed., 2003.

[2] J. Rabkowski, D. Peftitsis, and H.-P. Nee, "Silicon Carbide Power Transistors: A New Era in Power Electronics Is Initiated," *IEEE Ind. Electron. Mag.*, vol. 6, pp. 17–26, Jun. 2012.

[3] M. Chinthavali, P. Ning, Y. Cui, and L. M. Tolbert, "Investigation on the Parallel Operation of Discrete SiC BJTs and JFETs," in *Twenty-Sixth Annual IEEE Applied Power Electron. Conf. and Exp. (APEC)*, pp. 1076–1083, Mar. 2011.

[4] D. Peftitsis, R. Baburske, J. Rabkowski, J. Lutz, G. Tolstoy, and H.-P. Nee, "Challenges Regarding Parallel Connection of SiC JFETs," *IEEE Trans. Power Electron.*, vol. 28, pp. 1449–1463, Mar. 2013.

[5] J. Rabkowski, D. Peftitsis, M. Zdanowski, and H.-P. Nee, "A 6 kW, 200 kHz Boost Converter With Parallel-Connected SiC Bipolar Transistors," in *Twenty-Eighth Annual IEEE Applied Power Electron. Conf. and Exp. (APEC)*, pp. 1991–1998, Mar. 2013.

[6] D. P. Sadik, J. Colmenares, D. Peftitsis, J. K. Lim, J. Rabkowski, and H.-P. Nee, "Experimental Investigations of Static and Transient Current Sharing of Parallel-Connected Silicon Carbide MOSFETs," in *2013 15th Eur. Conf. on Power Electron. and Appl. (EPE)*, pp. 1–10, Sept. 2013.

[7] F. Xu, T. Han, D. Jiang, L. Tolbert, F. Wang, J. Nagashima, S. J. Kim, S. Kulkarni, and F. Barlow, "Development of a SiC JFET-Based Six-Pack Power Module for a Fully Integrated Inverter," *IEEE Trans. Power Electron.*, vol. 28, pp. 1464–1478, Mar. 2013.

[8] Lemmon, M. Mazzola, J. Gafford, and C. Parker, "Stability Considerations for Silicon Carbide Field-Effect Transistors," *IEEE Trans. Power Electron.*, vol. 28, pp. 4453–4459, Oct. 2013.

[9] S. Luryi, J. Xu, A. Zaslavsky, and C. M. Zetterling, *Silicon Carbide High Temperature Electronics – Is This Rocket Science?*, p. 424. Wiley-IEEE Press, 2013.

[10] R. W. Johnson, J. L. Evans, P. Jacobsen, J. R. Thompson, and M. Christo- pher, "The Changing Automotive Environment: High-Temperature Electro- nics," *IEEE Trans. Electron. Packag. Manuf.*, vol. 27, pp. 164–176, Jul. 2004.

[11] E. Cilio, J. Garret, J. Fraley, J. Hornberger, B. McPherson, R. Schupbach, and Lostetter, "High temperature electronics (> 485°C) for venus exploration," in *Forth International Planetary Probe Workshop*, 2006.

[12] K. Rajashekara and B. Akin, "A Review of Cryogenic Power Electronics Status and Applications," in *IEEE Int. Electric Machines Drives Conf. (IEMDC)*, pp. 899–904, May 2013.

[13] C. A. Luongo, P. J. Masson, T. Nam, D. Mavris, H. D. Kim, G. V. Brown, M. Waters, and D. Hall, "Next Generation More-Electric Aircraft: A Poten- tial Application for HTS Superconductors," *IEEE Trans. Appl. Supercond.*, vol. 19, pp. 1055–1068, Jun. 2009.

[14] C. E. Jones, P. J. Norman, S. J. Galloway, M. J. Armstrong, and A. M. Boll- man, "Comparison of Candidate Architectures for Future Distributed Propul- sion Aircraft," *IEEE Trans. Appl. Supercond.*, vol. 26, pp. 1–9, Sept. 2016.

[15] Agarwal, "Advances in SiC MOSFET performance," presented at the ECPE SiC & GaN Forum Potential of Wide Bandgap Semicond. Power Electron. Appl., Birmingham, U.K., 2011.

[16] R. Singh, D. C. Capell, A. R. Hefner, J. Lai, and J. W. Palmour, "High power 4H-SiC JBS rectifiers," *IEEE Trans. Electron Devices*, vol. 49, no. 11, pp. 2054–2063, Nov. 2002.

[17] AP´erez-Tom´as, P.Brosselard, J. Hassan,XJord`a, P. Godignon, M. Placidi, Constant, J. Mill´an, and J. P. Bergman, "Schottky versus bipolar 3.3 kV SiC diodes," *Semicond. Sci. Technol.*, vol. 23, pp. 125004-1–125004-7, 2008.

[18] Application Notes CPWR-TECH1, 2005, CPWR-AN01, Rev. A, 2002 [Online]. Available: www.cree.com/power

[19] (2013). [Online]. Available: www.infineon.com/sic

[20] (2013). [Online]. Available: http://www.genesicsemi.com/index.php/sicproducts/schottky

[21] FF600R12IS4 F Data Sheet (2007). [Online]. Available: www.infineon.com

[22] T. Funaki, J. C. Balda, J. Junghans, A. S. Kashyap, H. A. Mantooth, F. Barlow,T.Kimoto, andT.Hikihara, "Power conversion with SiC devices at extremely high ambient temperatures," *IEEE Trans. Power Electron.*, vol. 22, no. 4, pp. 1321–1329, Jul. 2007.

[23] P. Ning, F.Wang, and K. D. T. Ngo, "High-temperature SiC power module electrical evaluation procedure," *IEEE Trans. Power Electron.*, vol. 26, no. 11, pp. 3079–3083, Nov. 2011.

[24] R. Wang, D. Boroyevich, P. Ning, Z. Wang, F. Wang, P. Mattavelli, K. D. T. Ngo, and K. Rajashekara, "A high-temperature SiC three-phase AC-DC converter design for >100 ◦C ambient temperature," *IEEE Trans. Power Electron.*, vol. 28, no. 1, pp. 555–572, Jan. 2013.

[25] P. Godignon, X. Jord`a, M. Vellveh´ı, X. Perpi˜n`a, V. Banu, D. L´opez, J. Barbero, P. Brosselard, and S. Massetti, "SiC Schottky diodes for harsh environment space applications," *IEEE Trans. Ind. Electron.*, vol. 58, no. 7, pp. 2582–2590, Jul. 2011.

[26] V. Scarpa, U. Kirchner, R. Kern, and R. Gerlach, "New SiC thin-wafer technology paving theway of Schottky diodeswith improved performance and reliability," *Power Electron. Eur.*, no. 3, pp. 30–32, 2012.

[27] R. J. Callanan,A.Agarwal, A. Burk,M.Das, B.Hull, F. Husna, A. Powell, J. Richmond, S-H. Ryu, and Q. Zhang, "Recent progress in SiC DMOSFETs and JBS diodes at Cree," in *Proc. 34th Ind. Electron. Conf.*, 2008, pp. 2885–2890.

[28] B. A. Hull, M. K. Das, J. T. Richmond, J. J. Sumakeris, R. Leonard J. W. Palmour, and S. Leslie, "A 180 Amp/4.5 kV 4H-SiC PiN diode for high current power modules," in *Proc. Int. Symp. Power Semicond. Devices ICs*, 2006, pp. 277–280.

[29] H. Niwa, G. Feng, J. Suda, and T. Kimoto, "Breakdown characteristics of 12–20 kV-class 4H-SiC PiN diodes with improved junction termination structures," in *Proc. Int. Symp. Power Semicond. Devices ICs*, 2012, pp. 381–384.

[30] P. Zhang, G. T. Dang, F. Ren, H. Cho, K.-P. Lee, S. J. Pearton, J.-I. Chyi, T.-Y. Nee, and C.-C. Chuo, "Comparison of GaN P-I-N and Schottky rectifier performance," *IEEE Trans. Electron. Devices*, vol. 48, no. 3, pp. 407–411, Mar. 2001.

[31] P. Zhang, J. W. Jonson, F. Ren, J. Han, A. Y. Polyakov, N. B. Smirnov, V. Govorkov, J. M. Redwing, K. P. Lee, and S. J. Pearton, "Lateral Al*x* Ga1−*x*N power rectifiers with 9.7 kV reverse breakdown voltage," *Appl. Phys. Lett.*, vol. 78, pp. 823–825, 2001.

[32] (2010) [Online]. Available: http://www.powdec.co.jp/Diode.pdf

[33] M. Placidi, A. P´erez-Tom´as, A. Constant, G. Rius, N. Mestres, J. Mill´an, and P. Godignon, "Effects of cap layer on ohmic Ti/Al contacts to Si+ implanted GaN," *Appl. Surface Sci.*, vol. 255, pp. 6057–6060, 2009.

[34] Fontser`e, A. P´erez-Tom´as, V. Banu, P. Godignon, J. Mill´an, H. De Vleeschouwer, J. M. Parsey, and P.Moens, "A HfO2 based 800 V/300 ◦C Au-freeAlGaN/GaN-on-SiHEMT technology," in *Proc. Int. Symp. Power Semicond. Devices ICs*, 2012, pp. 37–40.

[35] R. L. Kelley, M. Mazzola, S. Morrison, W. Draper, I. Sankin, D. Sheridan, and J. Casady, "Power Factor Correction Using an Enhancement-Mode SiC JFET," in *IEEE Power Electron. Specialists Conf.*, pp. 4766–4769, Jun. 2008.

[36] Q. Zhang, R. Callanan, M. K. Das, S. H. Ryu, A. K. Agarwal, and J. W. Palmour, "SiC Power Devices for Microgrids," *IEEE Trans. Power Electron.*, vol. 25, pp. 2889–2896, Dec. 2010.

[37] H. Zhang and L. M. Tolbert, "Efficiency Impact of Silicon Carbide Power Electronics for Modern Wind Turbine Full Scale Frequency Converter," *IEEE Trans. Ind. Electron.*, vol. 58, pp. 21–28, Jan. 2011.

[38] M. Chinthavali, L. M. Tolbert, and B. Ozpineci, "SiC GTO Thyristor Model for HVDC Interface," in *IEEE Power Eng. Soc. General Meeting*, vol. 1, pp. 680–685, Jun. 2004.

[39] D. Peftitsis, G. Tolstoy, A. Antonopoulos, J. Rabkowski, J. K. Lim, M. Bakowski, L. Ängquist, and H.-P. Nee, "High-Power Modular Multilevel Converters With SiC JFETs," *IEEE Trans. Power Electron.*, vol. 27, pp. 28– 36, Jan. 2012.

[40] L. Wu, J. Qin, M. Saeedifard, O. Wasynczuk, and K. Shenai, "Efficiency Evaluation of the Modular Multilevel Converter Based on Si and SiC Switch- ing Devices for Medium/High-Voltage Applications," *IEEE Trans. Electron Devices*, vol. 62, pp. 286–293, Feb. 2015.

[41] F. Xu, B. Guo, L. M. Tolbert, F. Wang, and B. J. Blalock, "An All-SiC Three- Phase Buck Rectifier for High-Efficiency Data Center Power Supplies," *IEEE Trans. Ind. Appl.*, vol. 49, pp. 2662–2673, Nov. 2013.

[42] Y. Hinata, M. Horio, Y. Ikeda, R. Yamada, and Y. Takahashi, "Full SiC Power Module With Advanced Structure and its Solar Inverter Applica- tion," in *Twenty-Eighth Annual IEEE Applied Power Electron. Conf. and Exp. (APEC)*, pp. 604–607, Mar. 2013.

[43] H. Akagi, T. Yamagishi, N. M. L. Tan, S. I. Kinouchi, Y. Miyazaki, and M. Koyama, "Power-Loss Breakdown of a 750–V 100–kW 20–kHz Bidirec- tional Isolated DC/DC Converter Using SiC MOSFET/SBD Dual Modules," IEEE Trans. Ind. Appl., vol. 51, pp. 420–428, Jan. 2015.

[44] G. Tolstoy, P. Ranstad, J. Colmenares, F. Giezendanner, and H.-P. Nee, "Experimental Evaluation of SiC BJTs and SiC MOSFETs in a Series-Loaded Resonant Converter," in 2015 17th Eur. Conf. on Power Electron. and Appl. (EPE), pp. 1–9, Sept. 2015.

[45] U. D. of Energy, "Wide Bandgap Semiconductors Pursuing the Promise," 2013.

[46] G. Kelner, M. Shur, S. Binari, K. Sleger, and H.-S. Kong, "High- Transconductance β-SiC Buried-Gate JFETs," IEEE Trans. Electron Devices, vol. 36, pp. 1045–1049, Jun. 1989. Bipin Patil, Alka Thakur, "Use of UPFC In Mitigating Harmonics From A 53kv Distribution Line", International Journal of Scientific Progress And Research (IJSPR), Volume 22, Number 03, 2016.